

GEOPHYSICAL SURVEY

CLAIM NAMES:

Mac, # P25031

64° 01' 08.25" NORTH

140° 44' 49.86" WEST

Map # 116C-02b

METHOD

GEOELECTRICAL RESISTIVITY TOMOGRAPHY (GRT)

FOR

Dredge Master Gold Ltd.

Dawson Mining District

AUTHORS

Stefan Ostermaier, Philipp Moll

Arctic Geophysics Inc.

WORK PERFORMED: September 13th - 14th 2008

DATE OF REPORT: Jan 08th 2009

Arctic Geophysics Inc.
Box 747, Dawson City, Y. T.
Y0B-1G0, Canada
Phone: 867-993-3671 (Cell)
01149-x781-474 9382 (Germany)
info@arctic-geophysics.com
www.arctic-geophysics.com



Table of Contents

1	Introduction.....	3
2	List of Claims.....	3
3	Location.....	3
4	Access.....	3
5	Work Method and Instrumentation.....	3
6	Work performed.....	4
6.1	Map.....	4
6.2	Glacier Creek 01.....	5
6.3	Glacier Creek 02	6
7	Geological implications.....	7
8	Recommendations.....	7
9	Data.....	8
9.1	Profile01.....	8
9.2	Profile02.....	15
10	Cost.....	23
11	Qualification.....	24
12	References.....	25

1 Introduction

This geophysical survey was conducted at *Glacier Creek* for the benefit of Dredge Master Gold Ltd..

The survey consists of two Geoelectrical Resistivity Tomography (GRT) profiles. The purpose of the survey was to determine the depth to bedrock on the placer claim MAC, #P25031.

2 List of Claims

Name	Grant Number	Owner
Mac	P25031	Dredge Master Gold Ltd.

3 Location

The claim is located near the confluence of Glacier Creek and Sixty Mile River on the western bank of the creek, map number 116C02.

4 Access

The claim can be accessed via a gravel road.

5 Work Method and Instrumentation

For this survey GEOELECTRICAL RESISTIVITY TOMOGRAPHY, GRT for short in the following article, was used.

The resistivity data acquisition used two-dimensional resistivity imaging equipment comprising of ACHERON 3.2,¹ an amplifier for the sender current, the 4-PUNKT-LIGHT² resistivity meter and a manual ELECTRODE SELECTOR SYSTEM.³ The Acheron 3.2 and 4-Punkt light were connected to 50 stainless steel electrodes, which were staked out on a straight line, with a constant spacing, via a MULTICORE CABLE⁴. The “Wenner equal spacing electrode array”, Wenner-array for short, was used for this survey. A dedicated software⁵ was used to select the four active electrodes for each measurement and to convert the measured data into a data format appropriate for the RES2DINV program.

The measured resistivity data was then interpreted with the RES2DINV⁶ inversion program.

Details about the survey and interpretation method can be found in published papers by Keller

¹Constructed and produced by Arctic Geophysics Inc.

²Constructed and produced by LGM (Germany)

³Constructed and produced by Arctic Geophysics Inc.

⁴Dito

⁵Developed by Stefan Ostermaier, Arctic Geophysics Inc.

⁶Geotomo Software (www.geoelectrical.com)

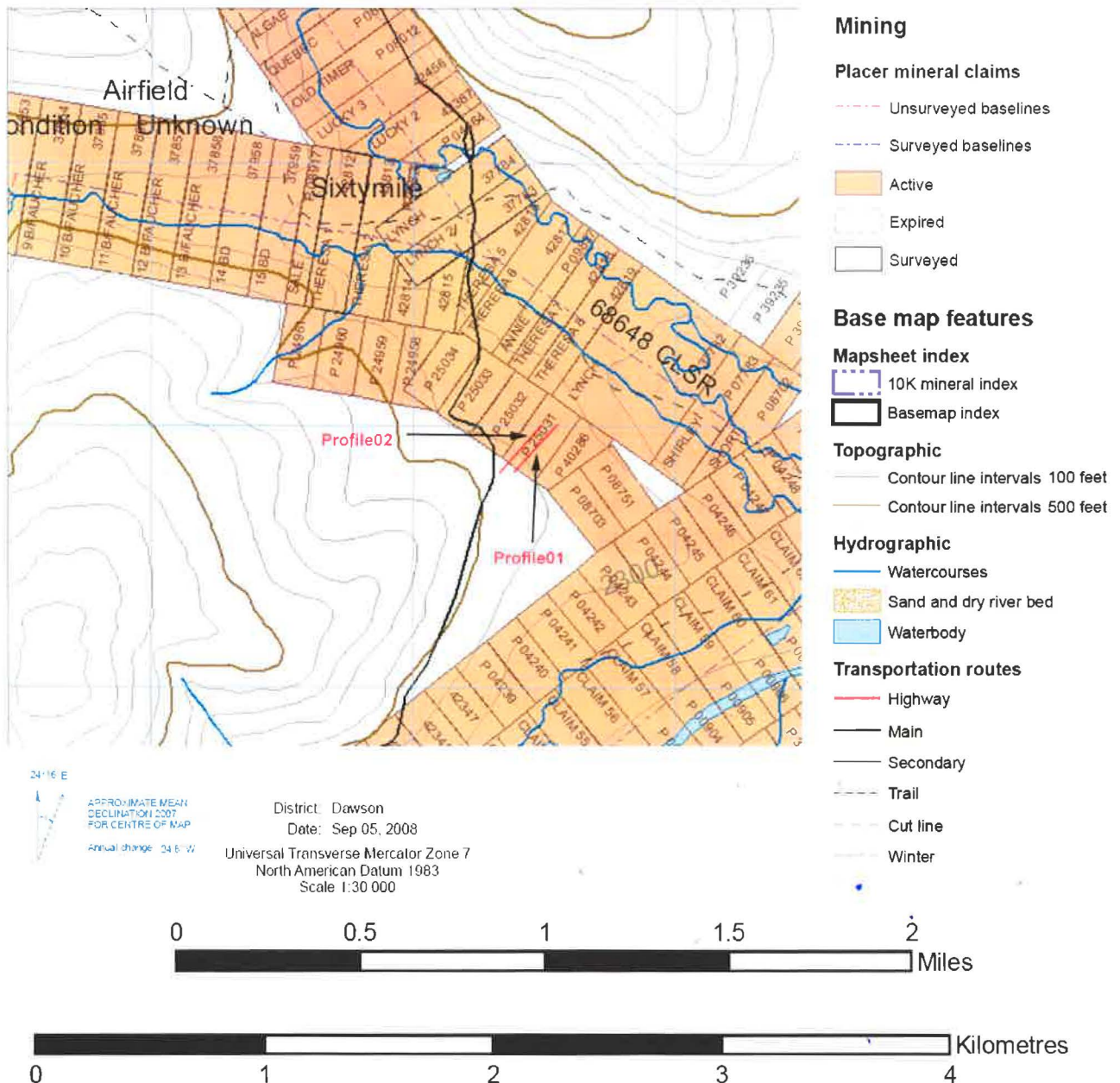
and Frischknecht, (1966), Griffiths *et al.*, (1990), Griffiths and Barker, (1993), and Loke and Barker (1996).

To interpret the resistivity data, a 2-D model for the subsurface consisting of a large number of rectangular blocks is generated by the software. The software then calculates the resistivity of each block so, that the calculated apparent resistivity and the measured apparent resistivity from the survey match.

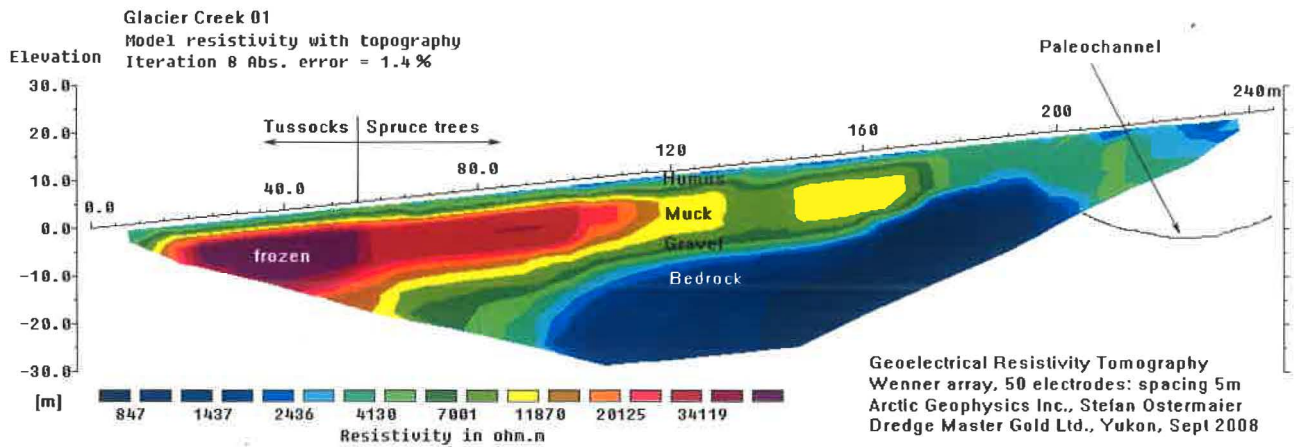
The RES2DINV program automatically subdivides the subsurface into a certain number of blocks, then it uses a least-squares inversion algorithm to determine the appropriate resistivity values for each block.

6 Work performed

6.1 Map



6.2 Glacier Creek 01



The Profile 01 shows the for the Sixty Mile area typical stratification of humus, muck, gravel and bedrock. On the left part the ground is frozen; the frost decreases towards the right side. The reason for this is the character of the vegetation: from 0 to 55m in the profile tussocks provide good insulation which preserves the permafrost. Above 55m in the profile there are less tussocks and more and more spruce trees. The decrease of insulation causes increased unfreezing, where the ground is still partially frozen up to 220m in the profile. This is supported by the resistivity values.⁷

Above 170m in the profile the stratification of the sediments is no longer detectable. It is possible that the discontinuous, partially thawed permafrost obscures the layers. However it is more likely that at this point a different kind of sediment begins: probably a mixture of mainly alluvial with colluvial gravel which have been stirred by down slope creep and deposited in the hypothetical channel above 200m in the profile.

Regardless of kind, structure and degree of permafrost of the sediment, we can see the border between sediment and bedrock throughout the profile. The bedrock (blue) has resistivity values of approximately 800 to 2000 Ωm depending on permafrost, the sediments (green to violet) on the other hand have higher resistivity values.⁸

Accordingly the transition from sediment to bedrock can be interpreted with a high degree of certainty: The bedrock is in the transition from the turquoise band (2040 Ωm) to the blue band (2886 Ωm). Towards the left edge of the profile the bedrock border becomes less clear due to the

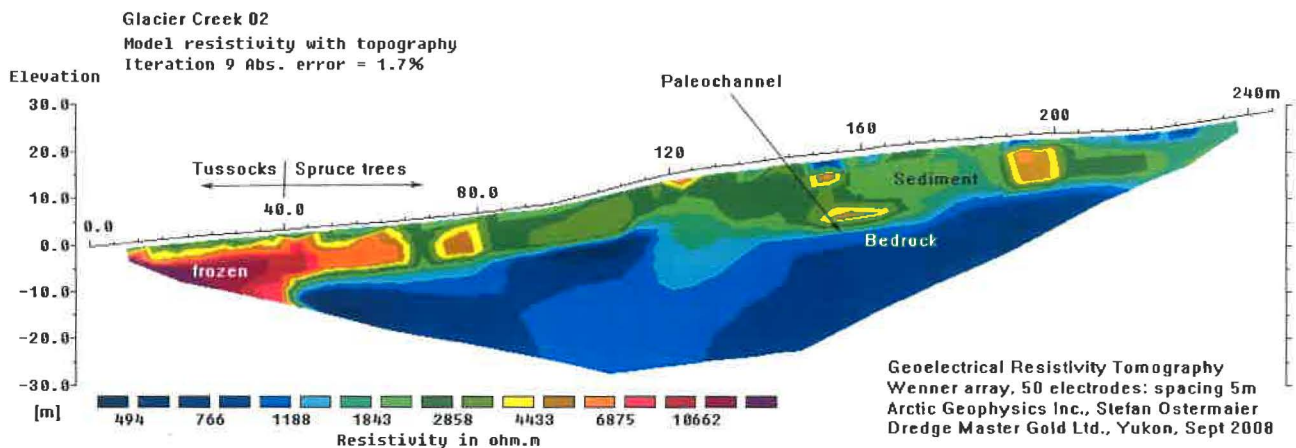
⁷ Frozen material has higher resistivity values, because ice is a nearly perfect insulator. The higher the amount of water in a given material the smaller is its conductivity when it is frozen.

⁸ When frozen the conductivity of sediments decreases more than that of solid rock, since the particles are insulated from each other by ice; in solid rock the mineral material stays in a stronger contact which reduces the decrease in conductivity. The more fine grained a sediment is the higher is the decrease in conductivity when frozen. Thus muck has in permafrost conditions usually markedly higher resistivity values compared to gravel. - In thawed conditions the reverse of this principle is true. High water content improves the conductivity of a material: hence muck (usually) is a better conductor than gravel, and gravel (usually) is a better conductor than rock. The variability of the conductivity contingent on water, is in solid rock rather inert, in sediments it increases with the reduction of particle size.

increase of frost and the tendency of the inversion program to slightly bend or round the edges of resistivity transitions. Still below 80m in the profile, an increase of the depth to bedrock must be considered probable. Above from 80m to 160m one can graphically determine bedrock at approximately 18m; this should correspond to 13m in reality.⁹

From 160m to 190m in the profile the bedrock grows shallower, until it reaches a depth of potentially only 6m (at 190m). Above 190m bedrock depth increases again. It is very probable that this is the beginning of a paleochannel! This hypothesis was investigated more thoroughly in Profile02.

6.3 Glacier Creek 02



Profile02 was made to further investigate the hypothetical paleochannel at the right hand side of Profile01. Accordingly the profile was done approximately 100m uphill and 50m upstream of Profile01. With overall less frost the transition from sediment to bedrock is shown in the contrast of the green and blue areas. The indentation in the bedrock between 120m and 180m in the profile corresponds, nearly without doubt, with the increase in bedrock depth at the right edge of the Profile01. This can be interpreted as a paleochannel with a high degree of certainty!¹⁰ The depth to bedrock is in reality most likely about 12m at the deepest point of the channel.

The sediment overlaying the bedrock is discontinuously frozen and not clearly stratified. Most likely it is a mixture of mainly alluvial with colluvial gravel and muck that has 'crept' downslope.

Let us take a closer look at the channel. In the interval 120-140m, less conductive material (turquoise: 1350 Ω m) reaches a greater depth. The bedrock underneath shows a higher resistivity than to both sides. It seems more water, which is now mainly frozen, has penetrated the ground

⁹ The Res2DInv-Program calculates layer borders usually a little deeper than they exist in reality. The necessary correctional factor is 60 to 100 % of the electrode spacing, depending on how high the transition between layers is. This empirical correctional factor was determined in numerous comparisons with drill profiles and shafts.

¹⁰ The existence of paleo channels at higher elevations has been confirmed in conversation with Laurie Downes and Mike McDougall.

at this place; the bedrock morphology would promote this. Increased erosion forms more openings for water to penetrate. The amount of fissures in the bedrock can also have been increased by tectonic processes which could be responsible for the angle of the channel. Water in rock fissures decreases the conductivity when frozen. All this leads to the supposition of a trench with higher weathering in the bedrock at 120 to 130m.

A second theory is, that it is possible for the dome like structure with less conductive bedrock material in the lower part of the channel to have been formed by a dike. All dikes we have reliably measured in the Yukon showed a conductivity less than the surrounding host rock.

7 Geological implications

The rocks in the Sixtymile district are known to be similar to those occurring in the Yukon River valley above Dawson. The beds have a general east and west strike. The bedrock at this location could be composed of the two broad bands of dark quartz-mica schists, quartzites and crystalline limestones reaching from Fortymile south to the Sixtymile.¹¹

8 Recommendations

The interpretations of Profile 01 and 02 suggests a depth to bedrock of 6 to 13m. The overlaying sediment is discontinuously frozen.

In this survey an old channel was located with a high likelihood: it is in Profile01 above 200m and in Profile02 between 120 and 180m. A paleochannel is an excellent target for placer mining. We recommend the verification of the paleochannel with further prospecting.

Variant 1: Drilling

Profile 01: at 190m, 220m, plus holes uphill until channel ends

Profile 02: at 100m, 120m, 160, 200m

Variant 2: Trenching

Profile 01: from 190m uphill

Profile 02: from 120m uphill

After successfully confirming the channel and confirming an economic amount of placer gold in the gravel we recommend a series of 2D Resistivity profiles along the valley. In this way the further progress of the channel can be efficiently mapped and it is also possible to detect adjacent channels.

When mining in the channel we recommend to check how deep the placer gold has penetrated into the possible bedrock fissures caused by weathering or tectonic processes.

¹¹ Yukon Placer Database 2007

9 Data

9.1 Profile01

50 Electrodes

Electrode spacing 5m

<i>A</i>	<i>M</i>	<i>N</i>	<i>B</i>	<i>I</i> [μ A]	<i>U</i> [μ V]	<i>Rho</i> [Ω m]
1	2	3	4	10	1518,1	4769,25
2	3	4	5	10	1606,7	5047,6
3	4	5	6	10	1632,2	5127,71
4	5	6	7	10	1594,6	5009,58
5	6	7	8	10	1961,7	6162,86
6	7	8	9	10	1543,6	4849,36
7	8	9	10	10	1887,4	5929,44
8	9	10	11	10	1695,5	5326,57
9	10	11	12	10	1941,4	6099,09
10	11	12	13	10	1871	5877,92
11	12	13	14	10	1970	6188,94
12	13	14	15	1	214,2	6729,29
13	14	15	16	10	1455,7	4573,22
14	15	16	17	1	207,1	6506,24
15	16	17	18	10	1557,7	4893,66
16	17	18	19	10	1852,1	5818,54
17	18	19	20	10	1360,6	4274,45
18	19	20	21	10	1594,7	5009,9
19	20	21	22	10	1427,1	4483,37
20	21	22	23	10	1127,3	3541,52
21	22	23	24	10	1257,2	3949,61
22	23	24	25	10	1237,3	3887,09
23	24	25	26	10	1059,8	3329,46
24	25	26	27	10	1502,1	4718,99
25	26	27	28	10	1011,8	3178,66
26	27	28	29	10	1215,4	3818,29
27	28	29	30	10	1189,3	3736,3
28	29	30	31	10	1149	3609,69
29	30	31	32	10	1073	3370,93
30	31	32	33	10	1033,9	3248,09
31	32	33	34	10	1082,6	3401,09
32	33	34	35	10	1162,9	3653,36
33	34	35	36	10	1088,1	3418,37
34	35	36	37	10	1116,1	3506,33
35	36	37	38	10	1101,8	3461,41
36	37	38	39	10	1138,7	3577,33
37	38	39	40	10	936,4	2941,79
38	39	40	41	10	1268,4	3984,8
39	40	41	42	10	773,4	2429,71
40	41	42	43	10	1201,5	3774,62
41	42	43	44	10	1003,7	3153,22
42	43	44	45	10	687,2	2158,9
43	44	45	46	10	999,7	3140,65
44	45	46	47	10	803	2522,7

A	M	N	B	I [μA]	U [μV]	Rho [Ωm]
45	46	47	48	10	825,5	2593,38
46	47	48	49	10	553,1	1737,61
47	48	49	50	10	909	2855,71
1	3	5	7	10	1348,9	8475,39
2	4	6	8	10	1341,4	8428,26
3	5	7	9	10	1482	9311,68
4	6	8	10	10	1408,5	8849,87
5	7	9	11	10	1478	9286,55
6	8	10	12	10	1525,1	9582,49
7	9	11	13	10	1540,6	9679,88
8	10	12	14	10	1484,1	9324,88
9	11	13	15	10	1602,7	10070,06
10	12	14	16	10	1660	10430,09
11	13	15	17	10	1428,5	8975,53
12	14	16	18	10	1294,3	8132,33
13	15	17	19	10	1437,2	9030,19
14	16	18	20	10	1339,4	8415,7
15	17	19	21	10	1126	7074,87
16	18	20	22	10	1204,8	7569,98
17	19	21	23	10	1260,1	7917,44
18	20	22	24	10	1064,8	6690,34
19	21	23	25	10	936,6	5884,83
20	22	24	26	10	951,5	5978,45
21	23	25	27	10	938,2	5894,88
22	24	26	28	10	989,8	6219,1
23	25	27	29	10	903,5	5676,86
24	26	28	30	10	722,6	4540,23
25	27	29	31	10	779,7	4899
26	28	30	32	10	892,2	5605,86
27	29	31	33	10	791,6	4973,77
28	30	32	34	10	687,4	4319,06
29	31	33	35	10	682,4	4287,65
30	32	34	36	10	757,3	4758,26
31	33	35	37	10	678,3	4261,88
32	34	36	38	10	595,4	3741,01
33	35	37	39	10	592,5	3722,79
34	36	38	40	10	617,1	3877,35
35	37	39	41	10	557,1	3500,36
36	38	40	42	10	483,5	3037,92
37	39	41	43	10	438,1	2752,66
38	40	42	44	10	533	3348,94
39	41	43	45	10	541,1	3399,83
40	42	44	46	10	398,6	2504,48
41	43	45	47	10	399,1	2507,62
42	44	46	48	10	550,4	3458,27
43	45	47	49	10	543,8	3416,8
44	46	48	50	10	328,5	2064,03
1	4	7	10	10	1227,9	11572,68
2	5	8	11	10	1205	11356,86
3	6	9	12	10	1248	11762,12
4	7	10	13	10	1190	11215,49
5	8	11	14	10	1206	11366,28
6	9	12	15	10	1230,6	11598,13
7	10	13	16	10	1314	12384,16

A	M	N	B	I [μ A]	U [μ V]	Rho [Ω m]
8	11	14	17	10	1344	12666,9
9	12	15	18	10	1229	11583,05
10	13	16	19	10	1220	11498,23
11	14	17	20	10	1052	9914,87
12	15	18	21	10	1070	10084,51
13	16	19	22	10	996,5	9391,79
14	17	20	23	10	1020	9613,27
15	18	21	24	10	923,7	8705,67
16	19	22	25	10	931,3	8777,3
17	20	23	26	10	797,9	7520,03
18	21	24	27	10	740,6	6979,99
19	22	25	28	10	725	6832,96
20	23	26	29	10	776,3	7316,46
21	24	27	30	10	694,3	6543,62
22	25	28	31	10	653,7	6160,98
23	26	29	32	10	578,4	5451,29
24	27	30	33	10	600,6	5660,52
25	28	31	34	10	552	5202,48
26	29	32	35	10	519,8	4899
27	30	33	36	10	464,3	4375,92
28	31	34	37	10	435	4099,78
29	32	35	38	10	425,4	4009,3
30	33	36	39	10	426,7	4021,55
31	34	37	40	10	399	3760,49
32	35	38	41	10	394,5	3718,07
33	36	39	42	10	348,8	3287,36
34	37	40	43	10	336,7	3173,32
35	38	41	44	10	303,5	2860,42
36	39	42	45	10	298,3	2811,41
37	40	43	46	10	284,4	2680,41
38	41	44	47	10	284	2676,64
39	42	45	48	10	274,3	2585,22
40	43	46	49	10	267,8	2523,96
41	44	47	50	10	289,8	2731,3
1	5	9	13	10	983	12352,74
2	6	10	14	10	917	11523,36
3	7	11	15	10	946	11887,79
4	8	12	16	10	982	12340,18
5	9	13	17	10	1015	12754,87
6	10	14	18	10	1069	13433,45
7	11	15	19	10	1035	13006,19
8	12	16	20	10	1012	12717,17
9	13	17	21	10	938	11787,26
10	14	18	22	10	847	10643,72
11	15	19	23	10	840	10555,75
12	16	20	24	10	784	9852,03
13	17	21	25	10	788	9902,3
14	18	22	26	10	703	8834,16
15	19	23	27	10	674,5	8476,02
16	20	24	28	10	632	7941,95
17	21	25	29	10	566	7112,57
18	22	26	30	10	606	7615,22
19	23	27	31	10	549	6898,94
20	24	28	32	10	526,3	6613,68

A	M	N	B	I [μA]	U [μV]	Rho [Ωm]
21	25	29	33	10	520	6534,51
22	26	30	34	10	435	5466,37
23	27	31	35	10	410,8	5162,27
24	28	32	36	10	359,9	4522,64
25	29	33	37	10	321	4033,8
26	30	34	38	10	310,7	3904,37
27	31	35	39	10	279	3506,02
28	32	36	40	10	276	3468,32
29	33	37	41	10	282	3543,72
30	34	38	42	10	277	3480,88
31	35	39	43	10	255	3204,42
32	36	40	44	10	256	3216,99
33	37	41	45	10	223	2802,3
34	38	42	46	10	213	2676,64
35	39	43	47	10	205	2576,11
36	40	44	48	100	1861	2338,6
37	41	45	49	100	1890	2375,04
38	42	46	50	100	1783	2240,58
1	6	11	16	10	758	11906,64
2	7	12	17	10	739	11608,18
3	8	13	18	10	787	12362,17
4	9	14	19	10	840	13194,69
5	10	15	20	10	806	12660,62
6	11	16	21	10	799	12550,66
7	12	17	22	10	805	12644,91
8	13	18	23	10	755	11859,51
9	14	19	24	10	655	10288,72
10	15	20	25	10	665	10445,8
11	16	21	26	10	606	9519,03
12	17	22	27	10	568	8922,12
13	18	23	28	10	540	8482,3
14	19	24	29	10	539	8466,59
15	20	25	30	10	571,3	8973,96
16	21	26	31	10	465,6	7313,63
17	22	27	32	10	454,5	7139,27
18	23	28	33	10	435	6832,96
19	24	29	34	10	392,5	6165,38
20	25	30	35	10	380,3	5973,74
21	26	31	36	10	316,5	4971,57
22	27	32	37	10	280	4398,23
23	28	33	38	10	249	3911,28
24	29	34	39	10	224	3518,58
25	30	35	40	10	204	3204,42
26	31	36	41	10	211	3314,38
27	32	37	42	10	201	3157,3
28	33	38	43	100	1956	3072,48
29	34	39	44	100	1935	3039,49
30	35	40	45	100	1931	3033,21
31	36	41	46	100	1762	2767,74
32	37	42	47	100	1690	2654,65
33	38	43	48	100	1634	2566,68
34	39	44	49	100	1404	2205,4
35	40	45	50	100	1356	2130
1	7	13	19	10	617	11630,18

A	M	N	B	I [μA]	U [μV]	Rho [Ωm]
2	8	14	20	10	629	11856,37
3	9	15	21	10	600	11309,73
4	10	16	22	10	644	12139,11
5	11	17	23	10	635	11969,47
6	12	18	24	10	618	11649,03
7	13	19	25	10	582	10970,44
8	14	20	26	10	503	9481,33
9	15	21	27	10	516	9726,37
10	16	22	28	10	465	8765,04
11	17	23	29	10	441	8312,65
12	18	24	30	10	413	7784,87
13	19	25	31	10	412	7766,02
14	20	26	32	10	405	7634,07
15	21	27	33	10	344	6484,25
16	22	28	34	10	344	6484,25
17	23	29	35	10	325	6126,11
18	24	30	36	10	303	5711,42
19	25	31	37	10	272	5127,08
20	26	32	38	10	223	4203,45
21	27	33	39	10	213	4014,96
22	28	34	40	100	1888	3558,8
23	29	35	41	100	1738	3276,05
24	30	36	42	100	1550	2921,68
25	31	37	43	100	1491	2810,47
26	32	38	44	100	1647	3104,52
27	33	39	45	100	1499	2825,55
28	34	40	46	100	1431	2697,37
29	35	41	47	100	1370	2582,39
30	36	42	48	100	1433	2701,14
31	37	43	49	100	1294	2439,13
32	38	44	50	100	1105	2082,88
1	8	15	22	10	478	10511,77
2	9	16	23	10	481	10577,74
3	10	17	24	10	488	10731,68
4	11	18	25	10	493	10841,64
5	12	19	26	10	461	10137,92
6	13	20	27	10	439	9654,11
7	14	21	28	10	406	8928,41
8	15	22	29	10	390	8576,55
9	16	23	30	10	366	8048,76
10	17	24	31	10	347	7630,93
11	18	25	32	10	332	7301,06
12	19	26	33	10	332	7301,06
13	20	27	34	10	301	6619,34
14	21	28	35	10	273	6003,58
15	22	29	36	10	254	5585,75
16	23	30	37	10	247	5431,81
17	24	31	38	10	224	4926,02
18	25	32	39	10	210	4618,14
19	26	33	40	100	1707	3753,89
20	27	34	41	100	1678	3690,11
21	28	35	42	100	1526	3355,85
22	29	36	43	100	1352	2973,2
23	30	37	44	100	1289	2834,66

A	M	N	B	I [μA]	U [μV]	Rho [Ωm]
24	31	38	45	100	1223	2689,52
25	32	39	46	100	1198	2634,54
26	33	40	47	100	1239	2724,7
27	34	41	48	100	1146	2520,19
28	35	42	49	100	1087,5	2391,54
29	36	43	50	100	1052	2313,47
1	9	17	25	10	381	9575,57
2	10	18	26	10	368	9248,85
3	11	19	27	10	361	9072,92
4	12	20	28	10	359	9022,65
5	13	21	29	10	344	8645,66
6	14	22	30	10	307	7715,75
7	15	23	31	10	314	7891,68
8	16	24	32	10	290	7288,49
9	17	25	33	10	278	6986,9
10	18	26	34	10	266	6685,31
11	19	27	35	10	255	6408,85
12	20	28	36	10	232	5830,8
13	21	29	37	10	211	5303,01
14	22	30	38	10	206	5177,34
15	23	31	39	100	1834	4609,34
16	24	32	40	100	1728	4342,94
17	25	33	41	100	1649	4144,39
18	26	34	42	100	1407	3536,18
19	27	35	43	100	1312	3297,42
20	28	36	44	100	1243	3124
21	29	37	45	100	1144	2875,19
22	30	38	46	100	1048	2633,91
23	31	39	47	100	1004	2523,33
24	32	40	48	100	1017	2556
25	33	41	49	100	938	2357,45
26	34	42	50	100	949	2385,1
1	10	19	28	10	288	8143,01
2	11	20	29	10	280	7916,81
3	12	21	30	10	274	7747,17
4	13	22	31	10	266	7520,97
5	14	23	32	10	244	6898,94
6	15	24	33	10	249	7040,31
7	16	25	34	10	233	6587,92
8	17	26	35	10	223	6305,18
9	18	27	36	10	210	5937,61
10	19	28	37	10	200	5654,87
11	20	29	38	100	1844	5213,79
12	21	30	39	100	1645	4651,13
13	22	31	40	100	1603	4532,38
14	23	32	41	100	1535	4340,11
15	24	33	42	100	1346	3805,73
16	25	34	43	100	1323	3740,69
17	26	35	44	100	1145	3237,41
18	27	36	45	100	1098	3104,52
19	28	37	46	100	993	2807,64
20	29	38	47	100	948	2680,41
21	30	39	48	100	900	2544,69
22	31	40	49	100	841	2377,87

A	M	N	B	I [μA]	U [μV]	Rho [Ωm]
23	32	41	50	100	822	2324,15
1	11	21	31	10	225	7068,58
2	12	22	32	10	217	6817,26
3	13	23	33	10	208	6534,51
4	14	24	34	100	1936	6082,12
5	15	25	35	100	1951	6129,25
6	16	26	36	100	1862	5849,65
7	17	27	37	100	1802	5661,15
8	18	28	38	100	1675	5262,17
9	19	29	39	100	1644	5164,78
10	20	30	40	100	1504	4724,96
11	21	31	41	100	1353	4250,57
12	22	32	42	100	1286	4040,09
13	23	33	43	100	1223	3842,17
14	24	34	44	100	1163	3653,67
15	25	35	45	100	1049	3295,53
16	26	36	46	100	926	2909,11
17	27	37	47	100	897	2818,01
18	28	38	48	100	857	2692,34
19	29	39	49	100	770	2419,03
20	30	40	50	100	748	2349,91
1	12	23	34	100	1729	5975
2	13	24	35	100	1641	5670,89
3	14	25	36	100	1517	5242,38
4	15	26	37	100	1578	5453,18
5	16	27	38	100	1481	5117,97
6	17	28	39	100	1429	4938,27
7	18	29	40	100	1389	4800,04
8	19	30	41	100	1350	4665,27
9	20	31	42	100	1251	4323,15
10	21	32	43	100	1108	3828,97
11	22	33	44	100	1077	3721,84
12	23	34	45	100	1006	3476,49
13	24	35	46	100	933	3224,22
14	25	36	47	100	895	3092,9
15	26	37	48	100	753	2602,18
16	27	38	49	100	745	2574,54
17	28	39	50	100	697	2408,66
1	13	25	37	100	1327	5002,67
2	14	26	38	100	1219	4595,52
3	15	27	39	100	1244	4689,77
4	16	28	40	100	1203	4535,2
5	17	29	41	100	1174	4425,88
6	18	30	42	100	1129	4256,23
7	19	31	43	100	1125	4241,15
8	20	32	44	100	1035	3901,86
9	21	33	45	100	934	3521,1
10	22	34	46	100	895	3374,07
11	23	35	47	100	839	3162,96
12	24	36	48	100	770	2902,83
13	25	37	49	100	730	2752,04
14	26	38	50	300	1961	2464,27
1	14	27	40	100	1005	4104,49
2	15	28	41	100	1017	4153,5

A	M	N	B	I [μA]	U [μV]	Rho [Ωm]
3	16	29	42	100	973	3973,8
4	17	30	43	100	963	3932,96
5	18	31	44	100	936	3822,69
6	19	32	45	100	913	3728,76
7	20	33	46	100	873	3565,39
8	21	34	47	100	776	3169,24
9	22	35	48	100	759	3099,81
10	23	36	49	100	700	2858,85
11	24	37	50	300	1942	2643,75
1	15	29	43	100	841	3698,91
2	16	30	44	100	801	3522,98
3	17	31	45	100	784	3448,21
4	18	32	46	100	767	3373,44
5	19	33	47	100	758	3333,86
6	20	34	48	100	721	3171,12
7	21	35	49	300	1990	2917,49
8	22	36	50	300	1892	2773,82
1	16	31	46	100	672	3166,73
2	17	32	47	300	1931	3033,21
3	18	33	48	300	1895	2976,66
4	19	34	49	300	1899	2982,94
5	20	35	50	300	1800	2827,43
1	17	33	49	300	1334	2235,14
2	18	34	50	300	1313	2199,95

9.2 Profile02

50 Electrodes

Electrode spacing 5m

A	M	N	B	I [μA]	U [μV]	Rho [Ωm]
1	2	3	4	10	1018,6	3200,03
2	3	4	5	10	1430,4	4493,73
3	4	5	6	10	1009,5	3171,44
4	5	6	7	10	1175,8	3693,88
5	6	7	8	10	1178,5	3702,37
6	7	8	9	10	839,3	2636,74
7	8	9	10	10	1459,3	4584,53
8	9	10	11	10	675,9	2123,4
9	10	11	12	10	1317,6	4139,36
10	11	12	13	10	834,2	2620,72
11	12	13	14	10	671,6	2109,89
12	13	14	15	10	1099,1	3452,92
13	14	15	16	10	771,4	2423,42
14	15	16	17	10	868,5	2728,47
15	16	17	18	10	743,8	2336,72
16	17	18	19	10	924,1	2903,15
17	18	19	20	10	658,5	2068,74
18	19	20	21	10	757,2	2378,81
19	20	21	22	10	798,2	2507,62
20	21	22	23	10	822,7	2584,59

A	M	N	B	I [μA]	U [μV]	Rho [Ωm]
21	22	23	24	10	876,4	2753,29
22	23	24	25	10	900,2	2828,06
23	24	25	26	10	719,7	2261
24	25	26	27	10	1107,4	3479
25	26	27	28	10	639,2	2008,11
26	27	28	29	10	955,1	3000,54
27	28	29	30	10	467,6	1469,01
28	29	30	31	10	769,5	2417,46
29	30	31	32	10	764,4	2401,43
30	31	32	33	10	239,2	751,47
31	32	33	34	10	1022,8	3213,22
32	33	34	35	10	349,7	1098,61
33	34	35	36	10	714,2	2243,73
34	35	36	37	10	672,4	2112,41
35	36	37	38	10	415,5	1305,33
36	37	38	39	10	651,8	2047,69
37	38	39	40	10	686,7	2157,33
38	39	40	41	10	423,1	1329,21
39	40	41	42	10	693,8	2179,64
40	41	42	43	10	652,7	2050,52
41	42	43	44	10	487,4	1531,21
42	43	44	45	10	698,2	2193,46
43	44	45	46	10	337	1058,72
44	45	46	47	10	617,4	1939,62
45	46	47	48	10	264,4	830,64
46	47	48	49	10	640,2	2011,25
47	48	49	50	10	457,3	1436,65
1	3	5	7	10	868,8	5458,83
2	4	6	8	10	855,8	5377,15
3	5	7	9	10	781,6	4910,94
4	6	8	10	10	727,3	4569,76
5	7	9	11	10	661,8	4158,21
6	8	10	12	10	663,3	4167,64
7	9	11	13	10	710,1	4461,69
8	10	12	14	10	597,3	3752,95
9	11	13	15	10	410,5	2579,25
10	12	14	16	10	483,1	3035,41
11	13	15	17	10	598,4	3759,86
12	14	16	18	10	416	2613,81
13	15	17	19	10	342,2	2150,11
14	16	18	20	10	417	2620,09
15	17	19	21	10	388,2	2439,13
16	18	20	22	10	333,9	2097,96
17	19	21	23	10	342,6	2152,62
18	20	22	24	10	368,7	2316,61
19	21	23	25	10	370	2324,78
20	22	24	26	10	310	1947,79
21	23	25	27	10	319,2	2005,59
22	24	26	28	10	381,9	2399,55
23	25	27	29	10	357,9	2248,75
24	26	28	30	10	321,3	2018,79
25	27	29	31	10	255,8	1607,24
26	28	30	32	10	393,4	2471,81
27	29	31	33	10	435,1	2733,81

A	M	N	B	I [μA]	U [μV]	Rho [Ωm]
28	30	32	34	10	276,3	1736,04
29	31	33	35	10	253,8	1594,67
30	32	34	36	10	322,4	2025,7
31	33	35	37	10	302,2	1898,78
32	34	36	38	10	303,6	1907,58
33	35	37	39	10	282,4	1774,37
34	36	38	40	10	294,3	1849,14
35	37	39	41	10	378,2	2376,3
36	38	40	42	10	269,4	1692,69
37	39	41	43	10	246,1	1546,29
38	40	42	44	10	316,5	1988,63
39	41	43	45	10	348,5	2189,69
40	42	44	46	10	247,3	1553,83
41	43	45	47	10	268,1	1684,52
42	44	46	48	10	253,7	1594,04
43	45	47	49	10	237,1	1489,74
44	46	48	50	10	216	1357,17
1	4	7	10	10	600	5654,87
2	5	8	11	10	507,1	4779,3
3	6	9	12	10	494,5	4660,55
4	7	10	13	10	473,2	4459,8
5	8	11	14	10	474,3	4470,17
6	9	12	15	10	383,6	3615,34
7	10	13	16	10	376,2	3545,6
8	11	14	17	10	298	2808,58
9	12	15	18	10	303,3	2858,54
10	13	16	19	10	299,8	2825,55
11	14	17	20	10	250,7	2362,79
12	15	18	21	10	227	2139,42
13	16	19	22	10	202,8	1911,34
14	17	20	23	10	211,3	1991,46
15	18	21	24	100	1949,3	1837,17
16	19	22	25	10	209,3	1972,61
17	20	23	26	100	1920,8	1810,31
18	21	24	27	100	1922,9	1812,29
19	22	25	28	100	1754,7	1653,77
20	23	26	29	10	224,2	2113,04
21	24	27	30	10	203,6	1918,88
22	25	28	31	100	1979,8	1865,92
23	26	29	32	100	1858,7	1751,78
24	27	30	33	100	1950,2	1838,02
25	28	31	34	10	222,1	2093,24
26	29	32	35	10	213,8	2015,02
27	30	33	36	100	1908,2	1798,44
28	31	34	37	100	1530,9	1442,84
29	32	35	38	100	1897,5	1788,35
30	33	36	39	100	1885,3	1776,85
31	34	37	40	10	224,2	2113,04
32	35	38	41	100	1908,6	1798,81
33	36	39	42	100	1944,3	1832,46
34	37	40	43	100	1705	1606,92
35	38	41	44	100	1623,8	1530,4
36	39	42	45	100	1659,5	1564,04
37	40	43	46	100	1606,4	1514

A	M	N	B	I [μA]	U [μV]	Rho [Ωm]
38	41	44	47	100	1920	1809,56
39	42	45	48	100	1735	1635,2
40	43	46	49	100	1664,7	1568,94
41	44	47	50	100	1308	1232,76
1	5	9	13	10	399	5013,98
2	6	10	14	10	341	4285,13
3	7	11	15	10	313	3933,27
4	8	12	16	10	321,8	4043,86
5	9	13	17	10	252,4	3171,75
6	10	14	18	10	260	3267,26
7	11	15	19	10	208	2613,81
8	12	16	20	100	1888,8	2373,54
9	13	17	21	10	207	2601,24
10	14	18	22	100	1551	1949,04
11	15	19	23	100	1435	1803,27
12	16	20	24	100	1391	1747,98
13	17	21	25	100	1321	1660,02
14	18	22	26	100	1234	1550,69
15	19	23	27	100	1312	1648,71
16	20	24	28	100	1287	1617,29
17	21	25	29	100	1316,8	1654,74
18	22	26	30	100	1370	1721,59
19	23	27	31	100	1219	1531,84
20	24	28	32	100	1413	1775,63
21	25	29	33	100	1271	1597,19
22	26	30	34	100	1394	1751,75
23	27	31	35	100	1455	1828,41
24	28	32	36	100	1115	1401,15
25	29	33	37	100	1377	1730,39
26	30	34	38	100	1195	1501,68
27	31	35	39	100	1094	1374,76
28	32	36	40	100	1511	1898,78
29	33	37	41	100	1226,7	1541,52
30	34	38	42	100	1460	1834,69
31	35	39	43	100	1510	1897,52
32	36	40	44	100	1080	1357,17
33	37	41	45	100	1232,5	1548,81
34	38	42	46	100	1017	1278
35	39	43	47	100	1060	1332,04
36	40	44	48	100	1252	1573,31
37	41	45	49	100	1115,3	1401,53
38	42	46	50	100	1061	1333,29
1	6	11	16	10	256	4021,24
2	7	12	17	10	235,5	3699,23
3	8	13	18	10	209	3282,96
4	9	14	19	100	1943	3052,06
5	10	15	20	100	1862*	2924,82
6	11	16	21	100	1451	2279,23
7	12	17	22	100	1417	2225,82
8	13	18	23	100	1389	2181,84
9	14	19	24	100	1131	1776,57
10	15	20	25	100	991	1556,66
11	16	21	26	100	1014	1592,79
12	17	22	27	100	957	1503,25

A	M	N	B	I [μA]	U [μV]	Rho [Ωm]
13	18	23	28	100	862	1354,03
14	19	24	29	100	976	1533,1
15	20	25	30	100	915	1437,28
16	21	26	31	100	928	1457,7
17	22	27	32	100	1025,5	1610,85
18	23	28	33	100	980	1539,38
19	24	29	34	100	956	1501,68
20	25	30	35	100	1023	1606,92
21	26	31	36	100	964	1514,25
22	27	32	37	100	862	1354,03
23	28	33	38	100	885	1390,15
24	29	34	39	100	873	1371,31
25	30	35	40	100	870	1366,59
26	31	36	41	100	895	1405,86
27	32	37	42	100	973	1528,38
28	33	38	43	100	955	1500,11
29	34	39	44	100	1003	1575,51
30	35	40	45	100	949	1490,69
31	36	41	46	100	872	1369,73
32	37	42	47	100	854	1341,46
33	38	43	48	100	817	1283,34
34	39	44	49	100	765	1201,66
35	40	45	50	100	776	1218,94
1	7	13	19	100	1668	3144,11
2	8	14	20	100	1732	3264,74
3	9	15	21	100	1400	2638,94
4	10	16	22	100	1386	2612,55
5	11	17	23	100	1090	2054,6
6	12	18	24	100	1072	2020,67
7	13	19	25	100	1096	2065,91
8	14	20	26	100	811	1528,7
9	15	21	27	100	791	1491
10	16	22	28	100	755	1423,14
11	17	23	29	100	786	1481,58
12	18	24	30	100	679	1279,88
13	19	25	31	300	1924	1208,88
14	20	26	32	100	795	1498,54
15	21	27	33	100	751	1415,6
16	22	28	34	100	783	1475,92
17	23	29	35	100	716	1349,63
18	24	30	36	100	748	1409,95
19	25	31	37	100	801	1509,85
20	26	32	38	300	1885	1184,38
21	27	33	39	300	1974	1240,3
22	28	34	40	300	1941	1219,57
23	29	35	41	100	708	1334,55
24	30	36	42	300	1982	1245,33
25	31	37	43	300	1790	1124,69
26	32	38	44	100	743	1400,52
27	33	39	45	100	730	1376,02
28	34	40	46	100	703	1325,12
29	35	41	47	100	685	1291,19
30	36	42	48	100	675	1272,35
31	37	43	49	100	705	1328,89

A	M	N	B	I [μA]	U [μV]	Rho [Ωm]
32	38	44	50	300	1770	1112,12
1	8	15	22	100	1303	2865,45
2	9	16	23	100	1120	2463,01
3	10	17	24	100	1041	2289,28
4	11	18	25	100	888	1952,81
5	12	19	26	100	809	1779,08
6	13	20	27	100	829	1823,07
7	14	21	28	100	691	1519,59
8	15	22	29	300	1933	1416,96
9	16	23	30	300	1908	1398,64
10	17	24	31	300	1672	1225,64
11	18	25	32	300	1722	1262,29
12	19	26	33	300	1784	1307,74
13	20	27	34	300	1819	1333,4
14	21	28	35	300	1825	1337,79
15	22	29	36	300	1674	1227,11
16	23	30	37	300	1791	1312,87
17	24	31	38	300	1809	1326,07
18	25	32	39	300	1613	1182,39
19	26	33	40	300	1629	1194,12
20	27	34	41	300	1524	1117,15
21	28	35	42	300	1514	1109,82
22	29	36	43	300	1661	1217,58
23	30	37	44	300	1499	1098,82
24	31	38	45	300	1451	1063,64
25	32	39	46	300	1621	1188,26
26	33	40	47	300	1623	1189,72
27	34	41	48	300	1706	1250,56
28	35	42	49	300	1663	1219,04
29	36	43	50	300	1451	1063,64
1	9	17	25	100	885	2224,25
2	10	18	26	100	857	2153,88
3	11	19	27	100	675	1696,46
4	12	20	28	300	1999	1674,68
5	13	21	29	100	686	1724,11
6	14	22	30	300	1696	1420,84
7	15	23	31	300	1568	1313,6
8	16	24	32	300	1585	1327,85
9	17	25	33	300	1481	1240,72
10	18	26	34	300	1482	1241,56
11	19	27	35	300	1499	1255,8
12	20	28	36	300	1438	1204,7
13	21	29	37	300	1348	1129,3
14	22	30	38	300	1430	1197,99
15	23	31	39	300	1445	1210,56
16	24	32	40	300	1346	1127,62
17	25	33	41	300	1393	1167
18	26	34	42	300	1248	1045,52
19	27	35	43	300	1270	1063,95
20	28	36	44	300	1259	1054,74
21	29	37	45	300	1286	1077,36
22	30	38	46	300	1218	1020,39
23	31	39	47	300	1240	1038,82
24	32	40	48	300	1285	1076,52

A	M	N	B	I [μA]	U [μV]	Rho [Ωm]
25	33	41	49	300	1240	1038,82
26	34	42	50	300	1342	1124,27
1	10	19	28	100	677	1914,17
2	11	20	29	300	1755	1654,05
3	12	21	30	300	1623	1529,64
4	13	22	31	300	1652	1556,97
5	14	23	32	300	1460	1376,02
6	15	24	33	300	1350	1272,35
7	16	25	34	300	1370	1291,19
8	17	26	35	300	1313	1237,47
9	18	27	36	300	1220	1149,82
10	19	28	37	300	1224	1153,59
11	20	29	38	300	1174	1106,47
12	21	30	39	300	1170	1102,7
13	22	31	40	300	1219	1148,88
14	23	32	41	300	1133	1067,83
15	24	33	42	300	1146	1080,08
16	25	34	43	300	1107	1043,32
17	26	35	44	300	1067	1005,62
18	27	36	45	300	1101	1037,67
19	28	37	46	300	1027	967,92
20	29	38	47	300	1111	1047,09
21	30	39	48	300	1071	1009,39
22	31	40	49	300	977	920,8
23	32	41	50	300	1063	1001,85
1	11	21	31	300	1404	1470,27
2	12	22	32	300	1432	1499,59
3	13	23	33	300	1393	1458,75
4	14	24	34	300	1245	1303,76
5	15	25	35	300	1146	1200,09
6	16	26	36	300	1177	1232,55
7	17	27	37	300	1135	1188,57
8	18	28	38	300	1044	1093,27
9	19	29	39	300	1017	1065
10	20	30	40	300	1062	1112,12
11	21	31	41	300	1076	1126,78
12	22	32	42	300	964	1009,5
13	23	33	43	300	962	1007,4
14	24	34	44	300	957	1002,17
15	25	35	45	300	984	1030,44
16	26	36	46	300	935	979,13
17	27	37	47	300	940	984,37
18	28	38	48	300	942	986,46
19	29	39	49	300	981	1027,3
20	30	40	50	300	870	911,06
1	12	23	34	300	1209	1392,67
2	13	24	35	300	1225	1411,1
3	14	25	36	300	1024	1179,56
4	15	26	37	300	1041	1199,15
5	16	27	38	300	1019	1173,8
6	17	28	39	300	974	1121,97
7	18	29	40	300	929	1070,13
8	19	30	41	300	947	1090,87
9	20	31	42	300	964	1110,45

A	M	N	B	I [μA]	U [μV]	Rho [Ωm]
10	21	32	43	300	866	997,56 .
11	22	33	44	300	884	1018,29
12	23	34	45	300	844	972,22
13	24	35	46	300	831	957,24
14	25	36	47	300	895	1030,97
15	26	37	48	300	839	966,46
16	27	38	49	300	842	969,91
17	28	39	50	300	834	960,7
1	13	25	37	300	1032	1296,85
2	14	26	38	300	943	1185,01
3	15	27	39	300	888	1115,89
4	16	28	40	300	925	1162,39
5	17	29	41	300	861	1081,96
6	18	30	42	300	849	1066,88
7	19	31	43	300	880	1105,84
8	20	32	44	300	814	1022,9
9	21	33	45	300	816	1025,42
10	22	34	46	300	769	966,35
11	23	35	47	300	792	995,26
12	24	36	48	300	789	991,49
13	25	37	49	300	769	966,35
14	26	38	50	300	760	955,04
1	14	27	40	300	842	1146,26
2	15	28	41	300	833	1134,01
3	16	29	42	300	797	1085
4	17	30	43	300	802	1091,81
5	18	31	44	300	788	1072,75
6	19	32	45	300	760	1034,63
7	20	33	46	300	762	1037,35
8	21	34	47	300	737	1003,32
9	22	35	48	300	740	1007,4
10	23	36	49	300	731	995,15
11	24	37	50	300	719	978,82
1	15	29	43	300	726	1064,37
2	16	30	44	300	760	1114,22
3	17	31	45	300	742	1087,83
4	18	32	46	300	688	1008,66
5	19	33	47	300	718	1052,64
6	20	34	48	300	706	1035,05
7	21	35	49	300	699	1024,79
8	22	36	50	300	691	1013,06
1	16	31	46	300	697	1094,85
2	17	32	47	300	670	1052,43
3	18	33	48	300	654	1027,3
4	19	34	49	300	657	1032,01
5	20	35	50	300	660	1036,73
1	17	33	49	300	627 .	1050,55
2	18	34	50	300	616	1032,12

10 Cost

QUANTITY	DESCRIPTION	AMOUNT
Transportation		
2	Van @ \$ 40.00 / day	\$ 80,00
Geophysical Survey		
2	Geoelectrical Resistivity Tomography Profiles @ \$ 600.00	\$ 1.200,00
1	Report @ \$ 200.00 for 1 st profile + \$ 50.00 for each additional profile	\$ 250,00
		<hr/>
		TOTAL \$ 1.530,00

11 Qualification

Stefan Ostermaier

- Study of geology, University of Freiburg, Germany
- Geophysical lectures and field courses, University of Karlsruhe and University of Stuttgart, Germany
- Study of computer science, University of Stuttgart, Germany
- Prospecting for precious metals and minerals in the Yukon, NWTs, and Alaska since 2001

Philipp Moll

- Study of geology, University of Freiburg, Germany
- Prospecting for precious metals and minerals in the Yukon, NWTs, and Alaska since 1989
- Geophysical lectures and field courses, University of Karlsruhe and University of Stuttgart, Germany
- Study of biology and German language and literature, University of Freiburg, Germany
- Apprenticeship of precision mechanic, Tools Factory Hermann Bilz, Zell, Germany



Stefan Ostermaier

Scientific Director, Arctic Geophysics Inc.



Philipp Moll

Managing Director, Arctic Geophysics Inc.

12 References

Chesterman W. Ch. and Lowe K.E.

Field Guide to Rocks and Minerals - North America, Chanticleer Press Inc. New York 2007

Evans A.M.

Erzlagerstättenkunde, Ferdinand Enke Verlag Stuttgart (1992)

Griffiths, D.H., Turnbull, J. and Olayinka, A.I.

Two dimensional resistivity mapping with a computer-controlled array, First Break 8: 121-129 (1990)

Griffiths, D.H. and Barker, R.D.

Two-dimensional resistivity imaging and modeling in areas of complex geology. Journal of Applied Geophysics 29 : 211 - 226. (1993)

Keller, G.V. and Frischknecht, F.C.

Electrical methods in geophysical prospecting. Oxford: Pergamon Press Inc. (1966)

Loke M.H. and Barker R.D.

Rapid least-squares inversion of apparent resistivity pseudosections by a quasi-Newton method. Geophysical Prospecting 44: 131-152 (1996)

Press F., Siever R., Grotzinger J., Thomas H.J.

Understanding Earth, W.H. Freeman and Company, New York (2004)

Robb L.

Introducing to Ore-Forming Processes, Backwell Science Ltd., 2005

Yukon Placer Database 2007, "<http://www.yukonminingrecorder.ca/>"

Yukon Placemap: 116C02P, "<http://www.yukonminingrecorder.ca/>"

["http://www.geology.gov.yk.ca/gallery/index.html"](http://www.geology.gov.yk.ca/gallery/index.html)